Locating Crack Tip in Mode-I Fracture Tests of Engineered Wood by Acoustic Emission and Machine Learning

XIANGDONG HE , PENG ZHANG and XUAN ZHU

ABSTRACT

As an eco-friendly construction material, engineered wood is becoming increasingly popular as it is environmentally friendly, less labor-intensive and more cost-effective compared with concrete and steel. On the other hand, compared with solid wood, layered engineered wood has more consistent mechanical properties, can minimize the influence of flaws like knots and get rid of the limitation of dimensions. Yet there is limited number of research focusing on the fracture behavior of layered engineered wood. This article investigates the fracture behavior of the laminated veneer lumber (LVL) via acoustic emission in mode-I fracture tests. The fracture test is conducted on an LVL sample with the help of six AE sensors to collect the AE waveforms. The difference of time of arrival is used to locate the crack tips. Since wood is highly heterogeneous, instead of using the wave velocity for AE source localization, this work leverages the benefits of probabilistic machine learning methods. Moreover, to capture the outliers more easily and being less sensitive to noise, a new type of probabilistic machine learning method, i.e., student-t process regression (STPR), is firstly proposed to address the AE source localization in mode-I fracture tests. As a comparison, the Gaussian process regression (GPR) is also implemented. Because not all AE events are related with the crack tip propagation, the Gaussian mixture models is implemented to identify AE events relevant with the crack tip. The results suggest STPR can outperform GPR both in pencil lead break test and in the mode-I fracture tests, only with the cost of having one additional parameter, i.e., the degree of freedom.

Xiangdong He, Peng Zhang, and Xuan Zhu, Department of Civil and Environmental Engineering, University of Utah, Salt Lake City, UT, 84112, U.S.A.

INTRODUCTION

As one of the oldest construction materials, wood has been widely used in civil engineering structures, such as bridges [1], towers [2], palaces [3], temples [4], and so on. However, the applications of solid wood have been limited due to inherent flaws and knots, which undermine the strength and result in inconsistent mechanical properties. Moreover, the dimension limitation restrains its use in large structural members. Industry and academia have been investigating engineered wood or mass timber as alternative construction materials that overcome the aforementioned limitations of solid wood [5–7]. Engineered wood is a broad class of wood products mainly referring to derivative wood products manufactured by binding or fixing the veneers, strands, particles, fibers, and so on with adhesives. For example, as one of the multi-layer engineered wood designs, laminated veneer lumber (LVL) has all its veneers. LVL has the strongest material properties along its longitudinal direction. Though LVL could be regarded as an orthotropic material [8], the inherent knots, internal voids, micro-cracks and potential inter-layer disbonds generally compromise such an assumption, resulting in a highly heterogeneous material [9]. Thus, it is important to understand their fracture behavior. As a technique to measure the fracture toughness of a material, which is an inherent material property, the mode-I fracture test can designate the crack to propagate along a desired direction.

Acoustic emission (AE) has been adopted to monitor damage evolution in mode-I fracture tests. As a passive nondestructive evaluation (NDE) and structural health monitoring (SHM) technique [10], the AE testing has been widely used for structural testing [11] and material characterization [12]. With the knowledge of wave velocity, AE sources could be located by analyzing the difference in time of arrival (dTOA) over different sensor pairs. Since AE testing can continuously monitor damage progress and track crack propagation, it is highly suitable for capturing and characterizing the fracture process in mode-I fracture tests. Many researchers [13–17] employed AE to estimate the mode-I fracture toughness of rocks. There are a few studies on using AE to monitor solid wood's damage progress and source localization in mode-I fracture tests.

There is little to no research focusing on using AE to monitor multi-layer engineered wood's fracture process in mode-I fracture tests. The challenges stem from material heterogeneity and complicated wave propagation paths, which would invalidate the wave velocity-based AE source localization methods. In this study, we develop the Student-t process regression (STPR) in this study, which is not only more robust to outliers due to the heavier-tailed distribution but also considers the influence of output on prediction variance. Based on these successful applications, it is reasonable to extend the Student-t process to AE source localization.

EXPERIMENTAL SETUPS

The test samples made of LVL were designed following the ASTM standards D5596 and D5045, and the sample dimension is shown in Figure 1(a). Two samples were prepared, both of which have the same configuration except the thicknesses: Sample 1 is 1.0 inch (in.) thick, and Sample 2 is 1.75 in. thick. As shown in Figure 1(a), a notch is set at the center of the sample with a length of 3.5 in.. The longitudinal axis is aligned with the horizontal direction and the X axis, while the tangential direction is

along the vertical direction and the Y direction. A region of interest (ROI) with a dimension of 4.0 in. × 0.5 in. and a grid size of 0.25 in., as shown in Figure 1(a) and (b), was defined on both sides of each sample. The mode-I fracture test setup is shown in Figure 1(c). A camera was placed in front of the loading frame to record the fracture process, which provides visual indications of crack tip propagation. The load frame was controlled by displacement with a loading rate of 0.5 mm/minute. Six AE sensors were mounted on the LVL samples, as shown in Figure 1(a) and 1(b).

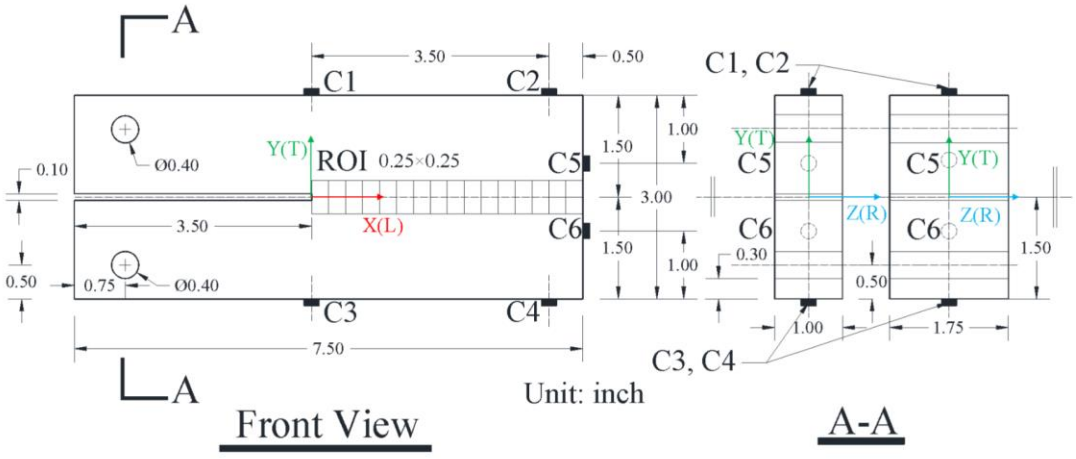

(a) Dimension of the two LVL samples

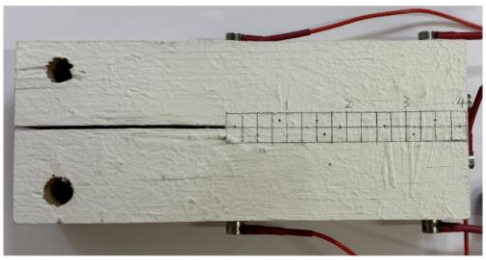

(b) LVL sample with defined Region of Interests

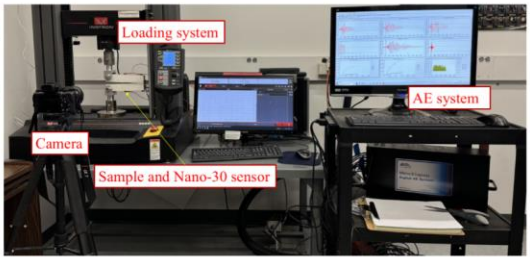

(c) The mode-I fracture test system

Figure 1. Experimental setup

By learning the difference in time of arrival or dTOA from different sensors, it is feasible to locate the source by triangular localization with the knowledge of wave velocity. But the heterogeneity of multi-layer engineered wood materials invalidates such an approach, and the machine learning method can potentially solve this problem. The training dataset for these models can be obtained by virtue of pencil lead breaking (PLB) tests, a technique widely used in the AE community to simulate AE signals. The PLB test provides a step function like transient force, which is very representative of real AE sources, and the generated waveform is remarkably reproducible. In light of that, multiple PLB tests were conducted to collect the dTOAs corresponding to each grid node within the ROI location on both LVL samples in this study. To estimate the AE source locations, a data bank needs to be first established. At least 10 pencil break tests were performed on each grid node. The time of arrival or TOA of each signal was extracted using the Akaike Information Criterion (AIC) method.

In the region of interest or ROI on both sides of a sample, PLB tests were first performed on every grid node to collect AE waveforms and build up the training dataset.

Meanwhile, PLB tests were conducted on ten off-grid nodes within the ROI. The TOA of each AE signal was determined by the AIC method, and dTOAs from all possible sensor pairs were calculated to construct the training dataset (based on PLB tests over on-grid nodes) and the testing dataset (based on PLB tests over off-grid nodes). Both training and testing datasets include dTOAs along with the corresponding X and Y coordinates. Consequently, the probabilistic machine learning or PML models were trained by minimizing the negative log-likelihood. Once the PLB tests were done and PML models were tuned, the mode-I fracture tests can be conducted, where the AE source locations are unknown. The AIC picker was used to determine the dTOAs in the fracture tests. With the tuned PML models via the PLB tests, predictions can be directly made on AE sources in the fracture tests. After this procedure, the final results were compared with the observations from the video camera.

AE SOURCE LOCALIZATION FOR PLB TESTS

AE source predictions of individual nodes on Sample 1 are shown in Figure 2. Each symbol type represents testing on a unique off-grid node: the red symbols are the ground truth, the blue ones are the mean predictions, and the black markers are the individual predictions. Clearly, the multi-output STPR demonstrates more compact results than single-output STPR. Moreover, both single-output and multi-output STPR can make accurate predictions for the points on the center line (Y=0). There are some deviations regarding the predictions on nodes away from the horizontal center line. For example, the predictions on the triangle in Figure 2(a), and predictions on the star in Figure 2(b) are away from the ground truth. These large errors could be attributed to internal defects within its neighboring areas, not using the optimal hyper-parameters, and errors from the data collecting and processing.

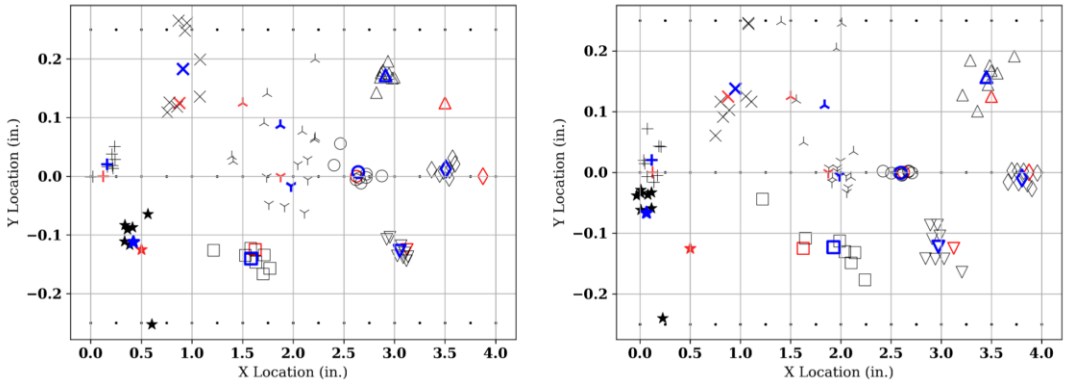

(a) Single-output STPR (b) Multi-output STPR

Figure 2. AE source localization from PLB tests on Sample 1, where ground truth is marked as red, individual prediction is marked as black, and mean predictions marked as blue.

In Figure 3, the blue symbols represent the mean predictions; the red ones are the ground truth, and the black ones are the individual predictions. Notably, the predictions along the X-axis (Y=0) are very accurate for both models. The multi-output STPR outperforms the single-output STPR. As shown in Figure 3(b), the multi-output STPR's predictions on the star, square, and inverted triangle are closer to the corresponding ground truth, which is not the case for single-output STPR predictions in Figure 3(a).

The enhanced performance of multi-output STPR again demonstrates the superiority of multi-output STPR and the necessity of considering the correlation between X and Y coordinates.

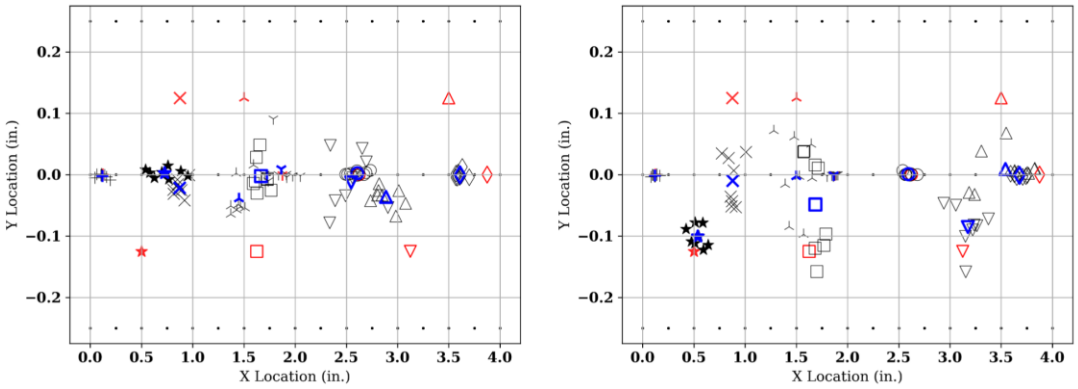

(a) Single-output STPR (b) Multi-output STPR

Figure 3. AE source localization from PLB tests on Sample 2, where ground truth is marked as red, individual prediction is marked as black, and mean predictions marked as blue.

AE SOURCE LOCALIZATION FOR MODE-I FRACTURE TESTS

The predictions of the crack tip locations throughout the fracture process of Sample 1 are shown in Figure 4(a) and 4(b) for the single-output and multi-output STPR, respectively. The red crosses are the predictions likely to be related to crack tip locations identified by Gaussian mixture model (GMM) clustering, while the green dots are other source location predictions likely not to be related to crack tip. In Figure 4, most of the crack tip locations are identified along the horizontal center line (Y=0), and this is true for the results of both models. Most of the crack tip locations are above Y=0, which is also true and backed up by the observations. According to camera footages, the crack propagates along the horizontal center line on the front. On the backside, however, the crack slightly propagated away from the center line to the upper part. No visible cracks were observed below Y=0 on Sample 1. This observation corresponds well to the localization results by STPR. In the meantime, the multi-output STPR predictions in Figure 4(b) are more compact than those by the single-output STPR in Figure 4(a). This again justifies the advantages of considering the correlation between the X and Y coordinates.

The results of the mode-I fracture test on Sample 2 over all stages are shown in Figure 5. The red crosses are the possible crack tip locations clustered by GMM from all the predictions, and the green dots represent locations from other sources. In Figure 17, most crack tip predictions are located along the horizontal center line. Based on the camera's observations from Sample 2, the crack developed along the X-axis with no obvious deviation. The crack tip predictions (red crosses) by multi-output STPR are tighter along Y=0 in Figure 5(b) than those by single-output STPR in Figure 5(a).

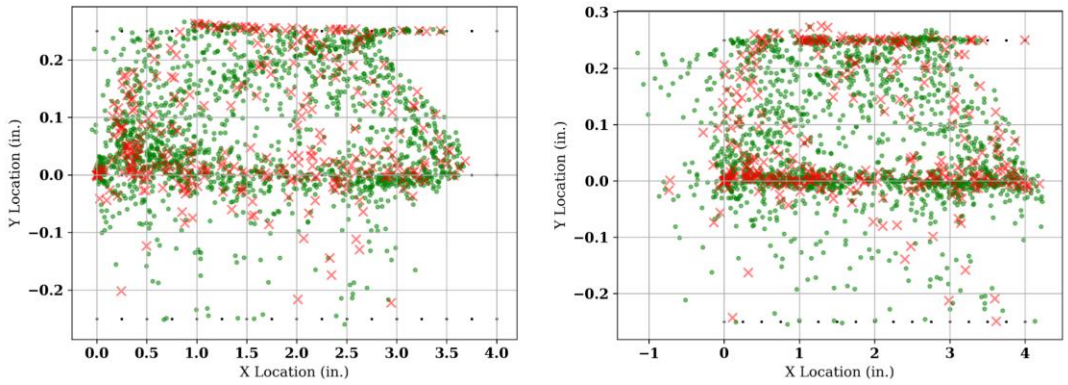

(a) Single-output STPR (b) Multi-output STPR

Figure 4. AE source localization from mode-I fracture test on Sample 1 by single-output and multi-output STPR. Red crosses: AE source likely to be related to crack tip propagation; green dots: others.

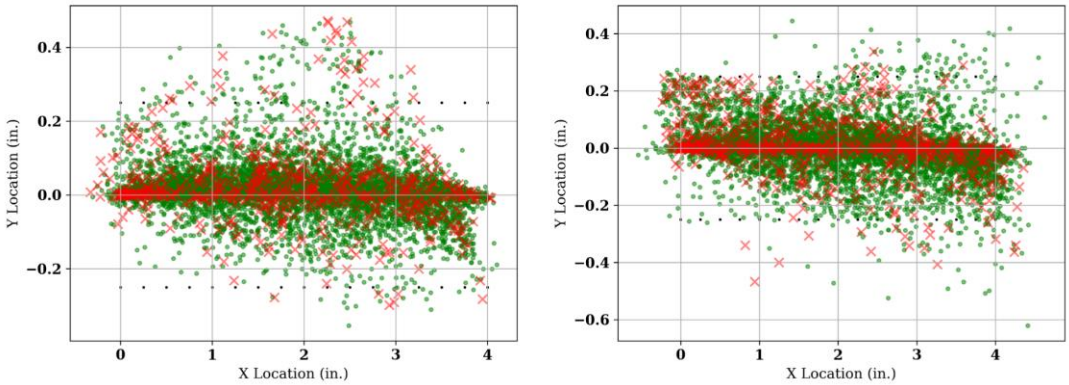

(a) Single-output STPR (b) Multi-output STPR

Figure 5. AE source localization from mode-I fracture test on Sample 2 by single-output and multi-output STPR. Red crosses: AE source likely to be related to crack tip propagation; green dots: others.

ACKNOWLEDGMENTS

The authors acknowledge financial support from Wood Innovations under USDA Grant 20-DG-11046000-615 and the startup package at the University of Utah. The authors appreciate the help from and discussion with Mr. Landon Oliver Van Amerongen on data collection.

REFERENCES

1. Pullin R, Holford KM, Lark RJ, Eaton MJ. 2008. “Acoustic emission monitoring of bridge structures in the field and laboratory.” *Journal of Acoustic Emission*. 26:172-81.
2. Carpinteri A, Lacidogna G. 2007. “Damage evaluation of three masonry towers by acoustic emission.” *Engineering structures*. 29(7):1569-79.
3. Johannesson C, Ljunggren S, Finney P. 1998. “Acoustic methods for locating fire spread paths in old buildings.” *NDT & E International*.1998;31(4):299-305.
4. Wu Y, Liu W, Li K. 2017. “A novel wireless acoustic emission sensor system for distributed wooden structural health monitoring.” *Int J Innov Comput Inf Control*.13(4):1289-306.
5. Harte AM. 2017. “Mass timber–the emergence of a modern construction material. Journal of Structural Integrity and Maintenance.” 2(3):121-32.
6. Ayanleye S, Udele K, Nasir V, Zhang X, Militz H. 2022. “Durability and protection of mass timber structures: A review.” *Journal of Building Engineering*. 46:103731.

7. Chen F, Li M, Li Z. 2024. “Self-centering mass timber structures: A review on recent research progress.” *Engineering Structures*. 303:117474.
8. Atreya N, Wang P, Zhu X. 2023. “Characterizing mechanical properties of layered engineered wood using guided waves and genetic algorithm.” Sensors. 23(22):9184.
9. He X, Zhu X. 2024 “Two-dimensional acoustic emission source localization on layered engineered wood by machine learning: a case study of laminated veneer lumber plate structure.” *Structural Health Monitoring*. 23(4):2423-42.
10. Grosse CU, Ohtsu M, Aggelis DG, Shiotani T. 2021. *Acoustic emission testing: Basics for research–applications in engineering*. Springer Nature.
11. He X, Williamson E, Wu Y, Briggs D, Zhu X, Pantelides CP. 2024. “Monitoring a mass timber—BRB braced mass timber frame under cyclic loading via acoustic emission.” *Structural Health Monitoring*.14759217241286049.
12. Giordano M, Calabro A, Esposito C, D’Amore A, Nicolais L. 1998. “An acoustic-emission characterization of the failure modes in polymer-composite materials.” *Composites science and technology*. 58(12):1923-8.
13. Nasseri M, Mohanty B, Young R. 2006. “Fracture toughness measurements and acoustic emission activity in brittle rocks.” *Pure and Applied Geophysics*. 163:917-45.
14. Du K, Li X, Tao M, Wang S. 2020. “Experimental study on acoustic emission (AE) characteristics and crack classification during rock fracture in several basic lab tests.” *International Journal of Rock Mechanics and Mining Sciences*. 133:104411.
15. Jiang R, Dai F, Liu Y, Li A, Feng P. 2021. “Frequency characteristics of acoustic emissions induced by crack propagation in rock tensile fracture.” *Rock Mechanics and Rock Engineering*. 54:2053-65.
16. Munoz-Ibanez A, Delgado-Martín J, Herbón-Penabad M, Alvarellos-Iglesias J. 2021. “Acoustic emission monitoring of mode I fracture toughness tests on sandstone rocks.” *Journal of Petroleum Science and Engineering*. 205:108906.
17. Zhao Y, Yuan Y, Wang C, Zheng K, Bi J. 2024. “The mode I fracture toughness and acoustic emission characteristics of hot dry rock under temperature effects.” *Engineering Fracture Mechanics*. 301:110047.